# On the Formation of the Sulfonate Ion from Hydrated Sulfur Dioxide

**Andreas F. Voegele,* Christofer S. Tautermann, Christine Rauch, Thomas Loerting, and Klaus R. Liedl***

*Department of Theoretical Chemistry, University of Innsbruck, Innrain 52a, A-6020 Innsbruck, Austria*

*Received: December 8, 2003; In Final Form: February 29, 2004*

In solutions of hydrated $SO_2$ it is well-known that both the bisulfite ion $HOSO_2^-$ and the sulfonate ion $HSO_3^-$ are present whereas the sulfonate form prevails in some salts. Here we show by ab initio and transition state theory considerations how the mechanism of sulfonate formation works. In aqueous solution, dissolved $SO_2$ first forms a bisulfite ion which is in a next step converted into the sulfonate ion. Direct formation of the sulfonate ion is kinetically hindered due to a very high reaction barrier for this process. Tautomerization of the bisulfite ion into the sulfonate ion is catalyzed by water molecules. Insight into this process is vital in understanding the formation of sulfonate salts upon crystallization from aqueous solution.

## 1. Introduction

Solutions of $SO_2$ are weakly acidic and primarily form two series of salts, namely, bisulfites ($HSO_3^-$) and sulfites ($SO_3^{2-}$). Since acid−base reactions of aqueous $SO_2$ solutions are important in several processes such as corrosion processes, formation of sulfur-containing aerosols or acid rain formation,[1−3] and also in salt formation upon crystallization, it is quite important to understand the $SO_2/H_2O$ system in detail. While the structure of the sulfite ion is well defined, there are two important tautomeric structures discussed with the constitution $HSO_3^-$. In one structure, the proton is attached to an oxygen atom yielding the bisulfite ion [$SO_2(OH)^-$], whereas in the second structure it is attached to the sulfur atom forming the sulfonate ion ($HSO_3^-$, see Scheme 1).[4]

NMR spectroscopic studies by Horner and Connick[4] determined the ratio between **3** and **4** in solution and revealed that the energy difference between both ions is small. These results were confirmed by ab initio studies of bisulfite and sulfonate in solution or in the solid state,[5,6] whereas Smith et al.[7] found that in water clusters the bisulfite ion is more stable than the sulfonate ion. The parent acids, sulfurous acid and sulfonic acid (see Scheme 1), have not yet been characterized in free form.[8−12] Sülzle et al.[13] synthesized sulfurous acid by dissociative ionization experiments. However, the molecule was very short-lived and only characterized in situ mass-spectroscopically, but it was never isolated.

Theoretical investigations aid experimental studies in getting better insight into complex systems.[14] The $SO_2-H_2O/H_2SO_3$ system and the corresponding deprotonated ions have been studied by several research groups. An ab initio study of Li and McKee[15] at a highly correlated level of theory revealed that at 298 K the standard state free energy $\Delta G°$ for the reaction $SO_2 + H_2O \rightarrow SO(OH)_2$ is 14.6 kcal mol$^{-1}$, which is in reasonable agreement with our findings in a recent study[16] also at a highly correlated level of theory. Bishenden and Donaldson[17] found a positive $\Delta G°$ in aqueous solution as well. In 1983, Strömberg et al.[5] studied the $HSO_3^-/SO_2OH^-$ system theoretically by Hartree−Fock, MCSCF, and force field methods. They investigated solid bisulfite salts, incorporating electrostatic effects for the crystal field and found that the energy difference between $SO_2OH^-$ and $HSO_3^-$ is small, so both ions could be present. Experimental studies showed the prevalence of the $HSO_3^-$ ion over $SO_2OH^-$ in certain salts as for instance in $RbHSO_3$ and $CsHSO_3$ where the latter form was not found.[18,19] Other salts as for instance $NaHSO_3$ form pyrosulfites ($Na_2S_2O_5 \cdot H_2O$) or mixtures between sulfonate and pyrosulfites as for instance in the potassium salt. However, in this study we concentrate on the formation of the sulfonates, whereas pyrosulfites will be the subject of a future study.

**SCHEME 1: Sulfonic Acid (1), Sulfurous Acid (2), Sulfonate Ion (3), Hydrogen Sulfite or Bisulfite Ion (4)**

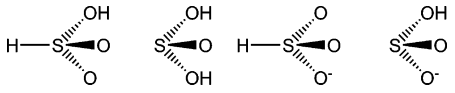


1 2 3 4

While the bisulfite ion and the sulfonate ion are both known to exist in solution,[4] the well-known autocatalytic effect of $H_2SO_3$ decomposition prevents existence of the acid molecule in an aqueous environment. Li and McKee[15] characterized the autocatalytic effect well showing that the decomposition of one $H_2SO_3$ molecule results in a water molecule that acts catalytically for further destruction. This catalytic effect has been quantified in terms of reaction barriers[15] and in more recent studies in terms of reaction rate constants by using variational transition state theory.[16,20,21] This catalytic effect not only accelerates the rate of decomposition but also explains why attempts to isolate sulfurous acid from aqueous $SO_2$ solutions failed. Sulfonic acid has been studied theoretically and was characterized to be even less stable,[14] so this molecule will be even more unlikely to exist in free form or in aqueous solution. Castleman and co-workers have studied protonated sulfur dioxide−water clusters experimentally and characterized them mass-spectroscopically.[22,23] Clusters of constitution $H_3SO_3^+$ indicated that $SO(OH)_2$ does not form in aqueous environment. Other studies investigated $SO_2$ and water mixtures showing the structure and stability of this complex.[24,25] In solution both the bisulfite salts and the sulfonate forms exist. Yet, in solids the prevalence of the sulfonate form has been shown in several salts.

* Corresponding authors. Tel.: +43-512-507-5147. Fax: +43-512-507-5144. E-Mail: Andreas.Voegele@uibk.ac.at, Klaus.Liedl@uibk.ac.at.

10.1021/jp0377578 CCC: $27.50 
Published on Web 04/06/2004

How the bisulfite and sulfonate form in solution has not yet been studied mechanistically. In this study, we demonstrate that the equilibration process between these two ions is a two-step mechanism. Starting from an $SO_2$ solution, the first step involves bisulfite formation whereas direct formation of the sulfonate is unlikely. The second step involves conversion of bisulfite into sulfonate, a process catalyzed by water molecules.

## 2. Methods

**2.1. Stationary Points.** Stationary points were calculated with hybrid density functional theory (DFT) B3LYP[26] with the 6-31+G(d) basis set and with Møller−Plesset perturbation Theory (MP2) and the 6-31G(d) basis set using the Gaussian98 program package.[27] Vibrational analysis confirmed the nature of these stationary points as minima or first-order saddle points. For optimization of the saddle points we employed the three-structure quadratic synchronous transit guided approach.[28] Since not only classical DFT but also hybrid DFT methods as B3LYP tend to underestimate reaction barriers,[29−32] we employed the Gaussian-3 approach to calculate energies at a higher, more accurate level of theory. In detail, we used the classical Gaussian-3 theory,[33] the Gaussian-3 theory using reduced Møller−Plesset order approach, G3(MP2),[34] and for some selected systems the recently developed modified Gaussian-3 approach of Baboul et al.[35] called G3//B3LYP as high level methods.[33,34] The G3//B3LYP (or G3B3) basis set extrapolation method uses B3LYP/6-31G(d) geometries for the single-point energy calculations at the higher levels of theory instead of MP2/6-31G(d) geometries as used in G3 and G3(MP2). Also vibrational frequencies and thus zero-point energy corrections are determined with B3LYP/6-31G(d) instead of HF/6-31G(d) as in G3. In both cases, the determined harmonic frequencies are scaled afterward correcting for anharmonic effects. These basis set extrapolation methods are all accurate within 1.7 kcal $mol^{-1}$ average absolute deviation compared to an experimental test set taken from the G2/97 set. This range of deviation has to be considered when discussing the results.

**2.2. Solvent Effects.** To describe solvent effects of the surrounding water environment we used a continuum approach to include these effects. In detail, we used the polarized continuum model (PCM) developed by Tomasi and co-worker (see refs 36−38 and references therein) with the default values as implemented in Gaussian98. The calculations were carried out at the B3LYP/6-31+G(d) level of theory. First, we re-optimized several of the gas-phase geometries using the PCM model obtaining optimized PCM energies. Then we performed single-point PCM energy calculations on the gas-phase structures and compared these results with the optimized PCM energies. We found that the difference is small in terms of energies and also very small in terms of geometries; thus, we used the single-point PCM energy calculations on the gas-phase structures because of the huge computational cost to reoptimize all structures and recalculate all reaction paths (see also results below). Finally, we employed the PCM corrections on our high level G3 calculations to obtain accurate barriers and reaction energies in solution.

**2.3. Reaction Path.** The reaction path was created—by starting from the transition state—as the steepest descent path in mass-scaled coordinates (scaling mass 1 amu). For creating this so-called minimum energy path (MEP) the Page-McIver local quadratic approximation algorithm[39] at a step size of 0.050 bohr (0.026 Å) was used in combination with B3LYP/6-31+G-(d). Distances on the potential energy surface from the transition state are denoted *s*, where *s* is positive on the product side and negative on the educt side. Every third point along the potential energy surface second derivatives and partition functions were calculated. The path was determined on both sides of the transition state until stable minimum structures were reached, i.e., when the gradient had almost vanished. B3LYP in general describes geometries and energy hypersurfaces well but underestimates the height of reaction barriers (as mentioned previously). Therefore, we interpolated the B3LYP/6-31+G(d) hypersurface to the energy values of the stationary points determined at the higher level G3 including solvent effect corrections. The interpolation procedure which is based on a logarithmic procedure is called variational transition state theory with interpolated corrections, and the shorthand notation is G3/// B3LYP/6-31+G(d).[40]

**2.4. Reaction Rates and Quantum Mechanical Tunneling.** Reaction rates were obtained using transition state theory (TST)[41] as implemented in Polyrate9.0[42] using Gaussrate9.0[43] as interface for Gaussian98. Theoretical details and equations can be found elsewhere;[41,44−50] here, we just briefly summarize the concepts. A variational approach for TST with a canonical ensemble was used to obtain a rate constant $k^{CVT}$ (CVT = canonical variational TST) minimized with respect to barrier crossings. When all bound degrees of freedom are described quantum-mechanically, motion along the reaction coordinate cannot be treated quantum-mechanically. Quantum mechanical effects along the reaction coordinate are treated in good approximation by semiclassical methods to evaluate transmission probabilities. Inclusion of the quantum mechanical effects on the reaction rate constant is carried out by multiplying the rate constant $k^{CVT}$ by a ground-state transmission coefficient $\kappa$. The transmission coefficient $\kappa$ is evaluated by different methods, which consider that the system tunnels along shorter paths in the course of the reaction that are more demanding in terms of energy. The methods we consider are the small curvature tunneling (SCT) approach by means of the centrifugal dominant small curvature semiclassical adiabatic ground-state tunneling method[51−53] and the large curvature tunneling (LCT) approach by the large curvature ground-state approximation version 4 (LCG4).[54] The approximation that best describes tunneling is determined according to the microcanonical optimized multi-dimensional tunneling ($\mu$OMT) method.

## 3. Results and Discussion

**3.1. Verification of the Methods.** *3.1.1. Gas-Phase Results.* The whole section 3.1 "Verification of the Methods" is intended as a justification for using the proposed methods. Results which are discussed in the following sections are presented, yet the underlying mechanisms together with the corresponding results will be described in the next sections. For the understanding of the paper, however, it is not vital to read section 3.1.

We used the tautomerization reactions of the bisulfite into the sulfonate ion as benchmark calculations to evaluate the most appropriate method to determine reaction barriers and reaction energies. These results are summarized in Tables 1 and 2. The corresponding mechanisms will be presented in the following sections. Barriers and reaction energies deviate by no more than 2 kcal $mol^{-1}$ (if not stated otherwise, the terms energies and barriers refer to electronic energy differences) at all used levels of theory within one type of reaction except for the reaction $SO_2OH^- \rightleftharpoons HSO_3^-$ where we observed an energy range of 4 kcal $mol^{-1}$. Since G3B3 and G3 energies are in good agreement, both B3LYP and MP2 geometries seem to be appropriate for determining the potential energy surface with these methods. However, calculation of all systems including the potential

**TABLE 1: Gas-Phase Reaction Barriers and Reaction Energies for Tautomerization Reactions at Different Levels of Theory. (The upper part of the table shows the tautomerization reaction of $SO_2OH^- \rightleftharpoons HSO_3^-$ (see Figure 2) whereas the lower part of the table shows the reaction $SO(OH)_2 \rightleftharpoons HSO_2OH$ (see Figure 3; in both cases the presence of water molecules has a catalyzing effect.)**

| | G3(MP2) | | G3 | | G3B3 | |
|---|---|---|---|---|---|---|
| | barrier | reaction *E* | barrier | reaction *E* | barrier | reaction *E* |
| | | | $SO_2OH^- + nH_2O \rightleftharpoons HSO_3^- + nH_2O$ | | | |
| $n = 0$ | 66.2 | −4.7 | 68.9 | −5.4 | 70.5 | −5.3 |
| $n = 1$ | 36.1 | −4.7 | 34.8 | −5.4 | 34.7 | −5.4 |
| $n = 2$ | 32.3 | −4.2 | 30.6 | −4.6 | 31.0 | −4.2 |
| | | | $SO(OH)_2 + nH_2O \rightleftharpoons HSO_2OH + nH_2O$ | | | |
| $n = 0$ | 101.6 | 7.6 | 101.1 | 6.6 | 101.7 | 6.9 |
| $n = 1$ | 38.6 | 10.0 | 37.3 | 9.4 | 37.0 | 13.7 |
| $n = 2$ | 28.7 | 11.0 | 27.3 | 11.4 | 27.1 | 11.6 |

**TABLE 2: Gas-Phase Reaction Barriers and Reaction Energies for the Hydration Reactions of $SO_2$ at Different Levels of Theory. (The upper part of the table shows the hydration mechanism forming $HSO_3H$, whereas the lower part of the table shows the energies for the hydration product $SO(OH)_2$. Both mechanisms are catalyzed by assisting water molecules as one can see from the mechanisms with $n = 2$ and $n = 3$.)**

| | G3(MP2) | | G3 | |
|---|---|---|---|---|
| | barrier | reaction *E* | barrier | reaction *E* |
| | | $SO_2 + nH_2O \rightleftharpoons HSO_3H + (n-1)H_2O$ | | |
| $n = 1$ | 69.1 | 15.7 | 68.2 | 14.5 |
| $n = 2$ | 48.6 | 18.8 | 46.8 | 17.8 |
| $n = 3$ | 36.4 | 18.2 | 34.5 | 17.2 |
| | | $SO_2 + nH_2O \rightleftharpoons SO(OH)_2 + (n-1)H_2O$ | | |
| $n = 1$ | 37.7 | 8.0 | 37.0 | 7.9 |
| $n = 2$ | 23.9 | 5.3 | 22.4 | 5.1 |
| $n = 3$ | 21.9 | 8.4 | 20.1 | 8.1 |

energy surfaces along the minimum energy paths is computationally demanding. To save computer time, we have chosen to consider the paths at the B3LYP/6-31+G(d) level of theory. For reaction barriers and energies we used the G3 results since these calculations were feasible for all systems and the results are within an acceptable error range.

*3.1.2. SCRF Calculations.* Next, we calculated the effects of the solvent on the energetics using a continuum model. We wanted to find out whether it is possible to use gas-phase geometries for the continuum calculations or whether it is necessary to use fully optimized geometries to evaluate the solvent effect. For this purpose we determined the structures of the reactants, transition states, and products for one representative reaction of each kind. This involved (1) the hydration of $SO_2$ yielding sulfonic acid, (2) the hydration of $SO_2$ yielding sulfurous acid, (3) the tautomerization of $SO(OH)_2$ into sulfonic acid, and (4) the tautomerization of $SO_2OH^-$ into the sulfonate ion. In each case, we investigated only the reactions without additional water molecules and determined the error when evaluating the solvent effect on the fully optimized geometry and the gas-phase geometry. These results are summarized in Table 3.

What can be seen from Table 3 is that the maximum error is below 0.8 kcal mol$^{-1}$ and that the maximum variation in bond length was determined to be around 0.02 Å. These small differences in the test calculations encouraged us to use the single-point energies for larger systems. Thus, for evaluating the energies in a simulated aqueous environment we calculated the energy difference between "solvated" and "unsolvated" species at the PCM B3LYP/6-31+G(d) level of theory and applied this "solvation correction" on the G3 energies. These results are summarized in Tables 4 and 5.

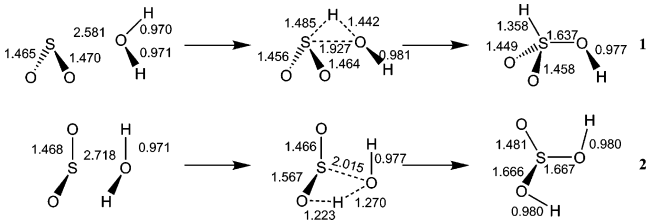


**Figure 1.** Pathways of $SO_2$ hydration. Mechanism **1** which yields sulfonic acid proceeds via a three-membered ring. Mechanism **2** yields sulfurous acid and proceeds via a four-membered ring. Both pathways involve a single deprotonation step in aqueous solution. (Distances are shown in Å.)

**TABLE 3: Difference between PCM Optimized Energies and PCM Energies on the B3LYP/6-31+G(d) Gas-Phase Geometries ($\Delta X = E_{PCM(opt)} - E_{PCM(g)}$) (The difference between the fully optimized B3LYP/6-31+G(d) PCM energies and the single-point PCM energies on the geometries obtained by B3LYP/6-31+G(d) is below 0.8 kcal mol$^{-1}$ for all test systems.)**

| reaction | Δbarrier [kcal mol$^{-1}$] | Δreaction *E* [kcal mol$^{-1}$] |
|---|---|---|
| $SO_2 + H_2O \rightarrow HSO_2OH$ | −0.32 | +0.56 |
| $SO_2 + H_2O \rightarrow SO(OH)_2$ | +0.52 | +0.23 |
| $HSO_2OH \rightarrow SO(OH)_2$ | −0.02 | +0.79 |
| $HSO_3^- \rightarrow SO_2OH^-$ | | +0.21 |

**TABLE 4: Reaction Barriers and Reaction Energies for Tautomerizations of $SO_2OH^-$ and $SO(OH)_2$, Respectively, in Simulated Aqueous Environment (The energies have been calculated from G3 energies applying PCM B3LYP/6-31+G(d) corrections.)**

| | barrier | reaction *E* |
|---|---|---|
| | $SO_2OH^- + nH_2O \rightleftharpoons HSO_3^- + nH_2O$ | |
| $n = 0$ | 76.0 | −11.5 |
| $n = 1$ | 22.1 | −10.1 |
| $n = 2$ | 21.8 | −11.8 |
| | $SO(OH)_2 + nH_2O \rightleftharpoons HSO_2OH + nH_2O$ | |
| $n = 0$ | 99.9 | 1.8 |
| $n = 1$ | 27.8 | 4.8 |
| $n = 2$ | 17.1 | 7.4 |

**TABLE 5: Reaction Barriers and Reaction Energies for the Hydration Reactions of $SO_2$ in Simulated Aqueous Environment (The energies have been calculated from G3 energies applying PCM B3LYP/6-31+G(d) corrections.)**

| | barrier | reaction *E* |
|---|---|---|
| | $SO_2 + nH_2O \rightleftarrows HSO_3H + (n-1)H_2O$ | |
| $n = 0$ | 68.6 | 13.0 |
| $n = 1$ | 38.3 | 12.8 |
| $n = 2$ | 24.1 | 12.8 |
| | $SO_2 + nH_2O \rightleftarrows SO(OH)_2 + (n-1)H_2O$ | |
| $n = 0$ | 42.5 | 11.1 |
| $n = 1$ | 23.3 | 5.1 |
| $n = 2$ | 19.2 | 8.8 |

**3.2. Hydration Mechanisms of $SO_2$.** Starting from solvated $SO_2$, there seem to be two possible pathways for $SO_2$ hydration. In the first pathway, $SO_2$ is formally hydrated via a three-membered transition state (TS) forming sulfonic acid (termed **1** in Figure 1). The deprotonation step will be after or during the hydration step. In gas-phase, the reaction barrier for this process is 68.2 kcal mol$^{-1}$ (energies used for discussion are the values determined at the G3 level of theory if not stated otherwise). When modeling the explicit interaction with water molecules (the remaining bulk being simulated as a polarizable continuum) where only one water molecule participates actively

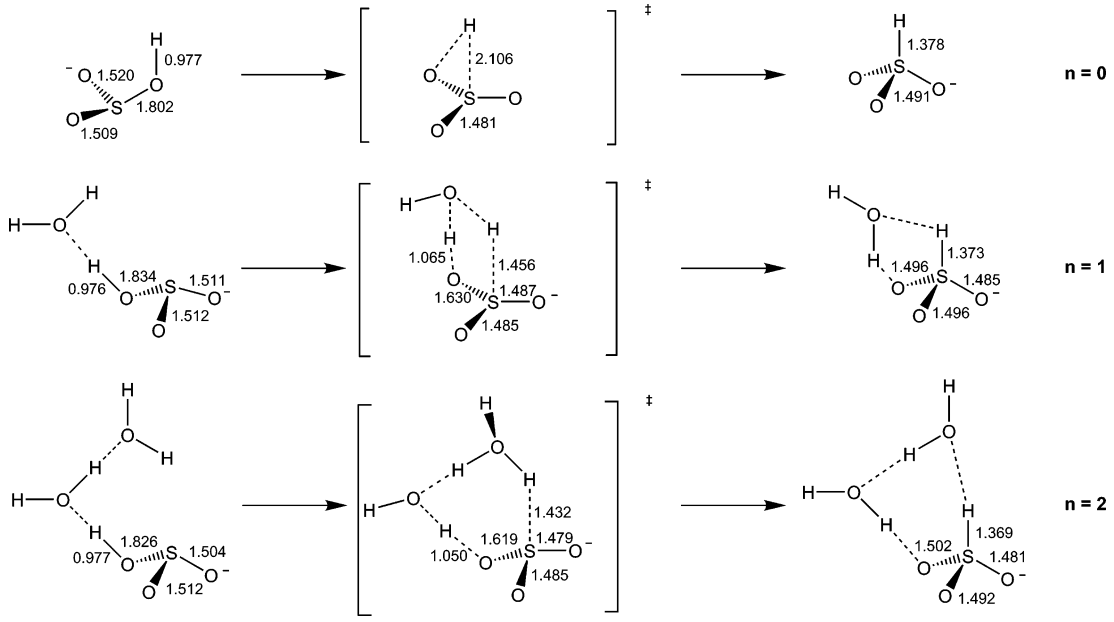


**Figure 2.** Tautomerization of the bisulfite into the sulfonate ion. Again, water molecules catalyze the reaction by releasing ring strain from the three-membered transition state as in mechanism $n = 1$.

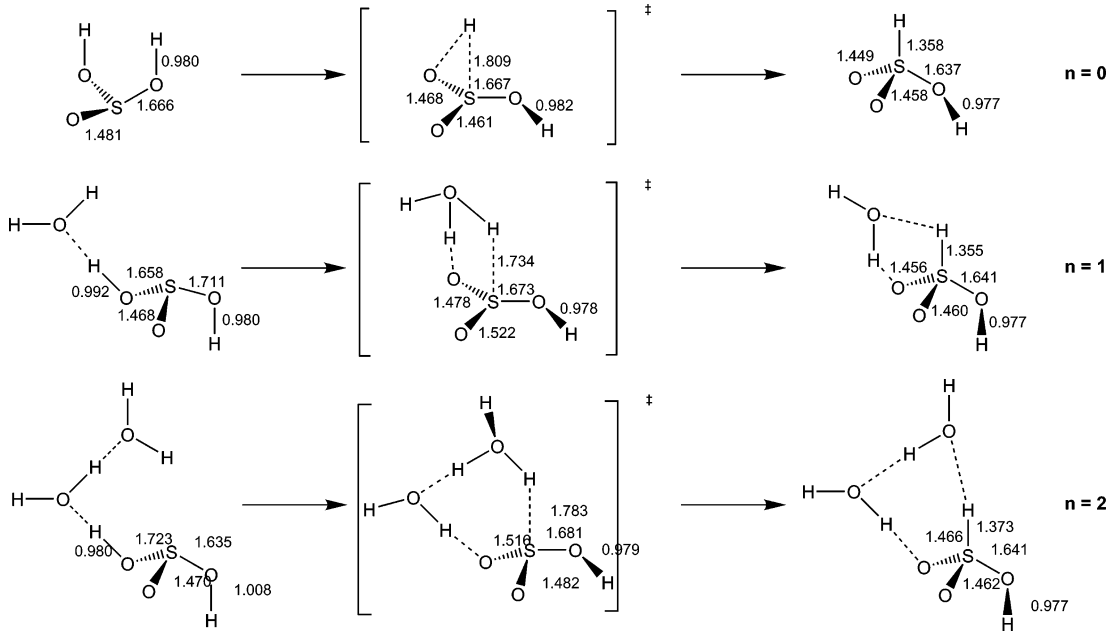


**Figure 3.** Tautomerization of sulfurous acid into sulfonic acid. Water molecules catalyze the reaction by releasing ring strain from the three-membered transition state as in mechanism $n = 1$.

in the mechanism, we did not observe a significant change in the geometry (see Supporting Information) and also the barrier remained almost constant. In the second pathway $SO_2$ is formally hydrated forming sulfurous acid (termed **2**) via a four-membered transition state ring, again involving a deprotonation step during or after hydration. The reaction barrier for this pathway in gas-phase is 37.0 kcal mol$^{-1}$, whereas in a continuum with again only one active water molecule the barrier is even higher. Three- or four-membered transition states suffer from high ring strain which is one reason reactions **1** and **2** are energetically unfavorable. However, including a second water molecule in the reactive ring increases the TS ring sizes from 3 to 5 and from 4 to 6, respectively. Such an expansion of the ring size usually releases much strain and thus one observes a reduction in the barrier height. In our case, a decrease to 46.8 kcal mol$^{-1}$ (**1**) and 22.4 kcal mol$^{-1}$ (**2**), respectively, was found. In a continuum model simulated aqueous environment the barrier of mechanism **1** catalyzed by one water molecule decreases by more than 8 kcal mol$^{-1}$ compared to gas-phase. A third active water molecule has an additional decreasing effect on the barriers lowering them to 36.4 and 20.1 kcal mol$^{-1}$ and to 26.1 and 19.2 kcal mol$^{-1}$ in solution. However, from these calculations is becomes clear that mechanism **2** is predominant both in gas-phase and in PCM simulated aqueous solution. Yet, from experiment we know that in solution both the sulfonate and the bisulfite ion exist in parallel and in some salts the sulfonate form predominates. Hence, there has to be an isomerization step that transforms the bisulfite ion into the sulfonate ion.

**3.3 Tautomerization of $HSO_3^-$/$SO_2OH^-$.** In Figure 2 we have highlighted the most likely pathways for the isomerization mechanisms of bisulfite into sulfonate; similarily sulfurous acid might be transformed into sulfonic acid (see Figure 3 even though the presence of one of the acid molecules in solution is

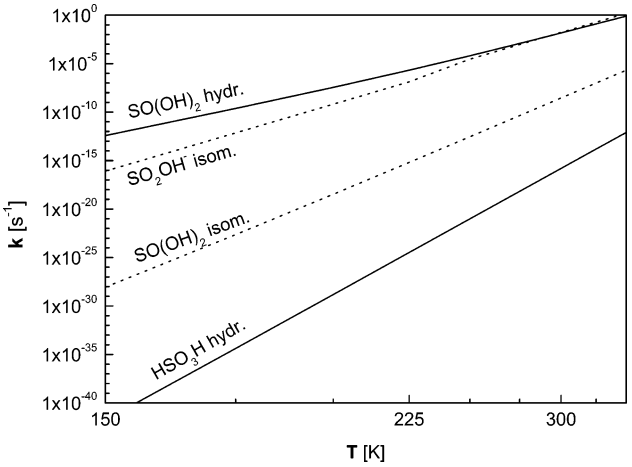


**Figure 4.** Reaction rate constants for the hydration of $SO_2$ into $SO(OH)_2$ and $HSO_3H$, respectively (- - -) and rate constants for the tautomerization of $SO_2OH^-$ into $HSO_3^-$ and of $SO(OH)_2$ into $HSO_3H$ (...).

unlikely). In solution the ionic form predominates and will thus be the main subject of the rest of our discussion.

The tautomerization process $SO_2OH^- \rightleftharpoons HSO_3^-$ proceeds via a three-membered transition structure ring with a reaction barrier of 76.0 kcal $mol^{-1}$ in solution. Including one and two water molecules in the reactive center, the barrier decreases to ca. 22 kcal $mol^{-1}$ in both cases. This enormous catalytic influence of additional water molecules lowers the time for equilibration quite remarkably since we determined a rate of $1.6 \times 10^{-2}$ $s^{-1}$ (the reaction rates of hydration and tautomerization are summarized in Figure 4 and a more detailed list of reaction rates and transmission coefficients summarizing quantum mechanical tunneling is summarized in Supporting Information). Yet, assuming that equilibration requires around 10 half-lives, which is a period of 8.5 min, this rate seems very reasonable. At room-temperature our calculations suggest that the effect of tunneling enhances the rate of conversion by around 30% due to tunneling effects. From a thermodynamic point of view, the $HSO_3^-$ ion is more stable than the $SO_2OH^-$ ion by several kcal $mol^{-1}$ both in gas-phase and in simulated solution, which is in good agreement with the computational findings of Brown and Barber,[6] Otto and Steudel,[14] and the experimental findings of Horner and Connick.[4] It remains unclear why Brown and Barber obtained lower reaction barriers.

As a conclusion, we find that starting from hydrated $SO_2$ the conversion into $HSO_3^-$ does not take place directly. In fact, the reaction barrier is too high and thus the rate constant is too slow for the hydration to the sulfonate, thus this step cannot take place. The mechanism of $HSO_3^-$ formation will most likely be a two-step process. First, $SO_2$ is hydrated forming the bisulfite ion $SO_2OH^-$. In the second step, $SO_2OH^-$ tautomerizes yielding the sulfonate ion $HSO_3^-$. Both steps are catalyzed by active water molecules. Additionally, the hydration and the tautomerization step are almost equally fast. Quantum mechanical tunneling plays an important role even in aqueous environment. Still one has to keep in mind the potential errors in the calculations. DFT calculations bear an error potential of several kcal $mol^{-1}$, therefore the energy differences might be smaller or larger than presented. However, previous studies showed the excellent performance of quantum mechanical studies on sulfur oxides and therefore we are confident in the presented mechanisms and results. Knowing the mechanism of $HSO_3^-$ formation is most important for understanding the equilibration process of $HSO_3^-/SO_2OH^-$ in aqueous solution and for understanding how salts of constitution $MeHSO_3$ form upon crystalization from solution.

**Acknowledgment.** This study was supported by the Austrian Science Fund (project number P14357-TPH).

**Supporting Information Available:** Cartesian coordinates of all structures as well as reaction rate constants and transmission coefficients of all reactions. This material is available free of charge via the Internet at http://pubs.acs.org.

## References and Notes

(1) Granat, L.; Rodhe, H.; Hallberg, R. O. In *Nitrogen, Phosphorus, and Sulfur*; Svensson, B. H., Søderlund, R., Eds.; Volume 32, Chapter: Global Cycles. Ecological Bulletins, Stockholm 1976.

(2) Graedel, T. E.; Crutzen, P. J. *Chemie der Atmosphäre, Bedeutung für Klima und Umwelt*; Spektrum, Akademischer Verlag: Heidelberg, Berlin, Oxford, 1994.

(3) Finlayson-Pitts, B. J.; Pitts, J. N., Jr. *Chemistry of the Upper and Lower Atmosphere*; Academic Press: San Diego-London, 2000.

(4) Horner, D. A.; Connick, R. E. *Inorg. Chem.* **1986**, *25*, 2414−2417.

(5) Strömberg, A.; Gropen, O.; Wahlgren, U.; Lindqvist, O. *Inorg. Chem.* **1983**, *22*, 1129−1133.

(6) Brown, R. E.; Barber, F. *J. Phys. Chem.* **1995**, *99*, 8071−8075.

(7) Smith, A.; Vincent, M. A.; Hillier, I. H. *J. Phys. Chem. A* **1999**, *103*, 1132−1139.

(8) Sanderson, R. T. *Inorganic Chemistry*; Reinhold Publishing Corporation: New York, Amsterdam, London, 1967.

(9) Lyons, D.; Nickless, G. In *Inorganic Sulphur Chemistry*; Nickless, G., Ed.; Elsevier Publishing Company: Amsterdam-London-New York, 1968; Chapter: The Lower Oxy-Acids of Sulphur, pp 509−533.

(10) Holleman, A. F. *Lehrbuch der anorganischen Chemie/Holleman−Wiberg*, volume 91.-100., verb. u. stark erw. Aufl./von Nils Wiberg. de Gruyter, Berlin-New York, 1985.

(11) Mortimer, C. E. *Chemistry*; Wadsworth Publishing: California, 1986.

(12) Greenwood, N. N.; Earnshaw, A. *Chemistry of the Elements*; Butterworth-Heinemann: Woburn, MA, 1997.

(13) Sülzle, D.; Verhoeven, M.; Terlouw, J. K.; Schwarz, H. *Angew. Chem., Int. Ed. Engl.* **1988**, *27*, 1533−1534.

(14) Otto, A. H.; Steudel, R. *Eur. J. Inorg. Chem.* **2000**, pp 617−624.

(15) Li, W.-K.; McKee, M. L. *J. Phys. Chem. A* **1997**, *101*, 9778−9782.

(16) Voegele, A. F.; Tautermann, C. S.; Loerting, T.; Hallbrucker, A.; Mayer, E.; Liedl, K. R. *Chem. Eur. J.* **2002**, *8*, 5644−5651.

(17) Bishenden, E.; Donaldson, D. J. *J. Phys. Chem. A* **1998**, *102*, 4638−4642.

(18) Simon, A.; Schmidt, W. *Z. Elektrochem.* **1960**, *64*, 737−741.

(19) Hayon, E.; Treinin, A.; Wilf, J. *J. Am. Chem. Soc.* **1972**, *94*, 47−57.

(20) Loerting, T.; Kroemer, R. T.; Liedl, K. R. *Chem. Commun.* **2000**, 999−1000.

(21) Loerting, T.; Liedl, K. R. *J. Phys. Chem. A* **2001**, *105*, 5137−5145.

(22) Castleman, A. W., Jr.; Bowen, K. H., Jr. *J. Phys. Chem.* **1996**, *100*, 12911−12944.

(23) Zhong, Q.; Hurley, S. M.; Castleman, A. W., Jr. *Int. J. Mass Spectrom.* **1999**, *185/186/187*, 905−911.

(24) Matsumura, K.; Lovas, F. J.; Suenram, R. D. *J. Chem. Phys.* **1989**, *91*, 5887−5894.

(25) Fleyfel, F.; Richardson, H. H.; Devlin, J. P. *J. Phys. Chem.* **1990**, *94*, 7032−7037.

(26) Stephens, P. J.; Devlin, F. J.; Chabalowski, C. F.; Frisch, M. J. *J. Phys. Chem.* **1994**, *45*, 11623−11627.

(27) Frisch, M. J.; Trucks, G. W.; Schlegel, H. B.; Scuseria, G. E.; Robb, M. A.; Cheeseman, J. R.; Zakrzewski, V. G.; Montgomery, J. A.; Stratmann, R. E.; Burant, J. C.; Dapprich, S.; Millam, J. M.; Daniels, A. D.; Kudin, K. N.; Strain, M. C.; Farkas, O.; Tomasi, J.; Barone, V.; Cossi, M.; Cammi, R.; Mennucci, B.; Pomelli, C.; Adamo, C.; Clifford, S.; Ochterski, J.; Petersson, G. A.; Ayala, P. Y.; Cui, Q.; Morokuma, K.; Malick, D. K.; Rabuck, A. D.; Raghavachari, K.; Foresman, J. B.; Cioslowski, J.; Ortiz, J. V.; Stefanov, B. B.; Liu, G.; Liashenko, A.; Piskorz, P.; Komaromi, I.; Gomperts, R.; Martin, R. L.; Fox, D. J.; Keith, T.; Al-Laham, M. A.; Peng, C. Y.; Nanayakkara, A.; Challacombe, M.; Gill, P. M. W.; Johnson, B.; Chen, W.; Wong, M. W.; Andres, J. L.; Gonzalez, C.; Head-Gordon, M.; Replogle, E. S.; Pople, J. A. *Gaussian 98, Revision A.9*; Gaussian, Inc.: Pittsburgh, PA, 1998.

(28) Peng, C.; Ayala, P. Y.; Schlegel, H. B. *J. Comput. Chem.* **1996**, *17*, 49−56.

(29) Durant, J. L. *Chem. Phys. Lett.* **1996**, *256*, 598−602.
(30) Jursic, B. S. *J. Mol. Struct. (THEOCHEM)* **1997**, *417*, 89−94.
(31) Lynch, B. J.; Fast, P. L.; Harris, M.; Truhlar, D. G. *J. Phys. Chem. A* **2000**, *104*, 4811−4815.
(32) Lynch, B. J.; Truhlar, D. G. *J. Phys. Chem. A* **2001**, *105*, 2936−2941.
(33) Curtiss, L. A.; Raghavachari, K.; Redfern, P. C.; Pople, J. A. *J. Chem. Phys.* **1998**, *109*, 7764−7776.
(34) Curtiss, L. A.; Redfern, P. C.; Raghavachari, K.; Rassolov, V.; Pople, J. A. *J. Chem. Phys.* **1999**, *110*, 4703−4709.
(35) Baboul, A. G.; Curtiss, L. A.; Redfern, P. C.; Raghavachari, K. *J. Chem. Phys.* **1999**, *110*, 7650−7657.
(36) Tomasi, J.; Persico, M. *Chem. Rev.* **1994**, *94*, 2027−2094.
(37) Barone, V.; Cossi, M.; Tomasi, J. *J. Comput. Chem.* **1998**, *19*, 404−417.
(38) Tomasi, J.; Cammi, R.; Mennucci, B.; Cappelli, C.; Corni, S. *Phys. Chem. Chem. Phys.* **2002**, *4*, 5697−5712.
(39) Page, M.; McIver, J. W., Jr. *J. Chem. Phys.* **1988**, *88*, 922−935.
(40) Chuang, Y.-Y.; Truhlar, D. G. *J. Phys. Chem. A* **1997**, *101*, 3808−3814.
(41) Eyring, H. *J. Chem. Phys.* **1935**, *3*, 107−115.
(42) Corchado, J. C.; Chuang, Y.-Y.; Fast, P. L.; Villá, J.; Hu, W.-P.; Liu, Y.-P.; Lynch, G. C.; Nguyen, K. A.; Jackels, C. F.; Melissas, V. S.; Lynch, B. J.; Rossi, I.; Coitiño, E. L.; Fernandez-Ramos, A.; Pu, J.; Albu, T. V.; Steckler, R.; Garrett, B. C.; Isaacson, A. D.; Truhlar, D. G. *Polyrate9.0*. University of Minnesota, Minneapolis, 2002.
(43) Corchado, J. C.; Chuang, Y.-Y.; Coitiño, E. L.; Truhlar, D. G. *Gaussrate9.0*. University of Minnesota, Minneapolis, 2002.
(44) Truhlar, D. G.; Hase, W. L.; Hynes, J. T. *J. Phys. Chem.* **1983**, *87*, 2664−2682.
(45) Truhlar, D. G.; Garrett, B. C. *Annu. Rev. Phys. Chem.* **1984**, *35*, 159−189.
(46) Truhlar, D. G.; Isaacson, A. D.; Garrett, B. C. In *Theory of Chemical Reaction Dynamics*; Baer, M., Ed.; CRC Press: Boca Raton, FL, 1985; Chapter: Generalized Transition State Theory, pp 65−137.
(47) Kreevoy, M. M.; Truhlar, D. G. In *Investigation of Rates and Mechanisms of Reactions*; Bernasconi, C. F., Ed.; John Wiley & Sons: New York, 1986; Chapter: Transition State Theory, pp 13−95.
(48) Tucker, S. C.; Truhlar, D. G. In *New Theoretical Concepts for Understanding Organic Reactions*; Bertrán, J., Csizmadia, I. G., Eds.; Kluwer: Dordrecht, The Netherlands, 1989; Chapter: Dynamical Formulation of Transition State Theory: Variational Transition States and Semiclassical Tunneling, pp 291−346. NATO ASI Series C 267.
(49) Truhlar, D. G. In *The Reaction Path in Chemistry: Current Approaches and Perspectives*; Heidrich, D., Ed.; Kluwer: Dordrecht, 1995; Chapter: Direct Dynamics Method for the Calculation of Reaction Rates, pp 229−255.
(50) Truhlar, D. G.; Garrett, B. C.; Klippenstein, S. J. *J. Phys. Chem.* **1996**, *100*, 12771−12800.
(51) Marcus, R. A.; Coltrin, M. E. *J. Chem. Phys.* **1977**, *67*, 2609.
(52) Skodje, R. T.; Truhlar, D. G.; Garrett, B. C. *J. Phys. Chem.* **1981**, *85*, 3019−3023.
(53) Baldridge, K. K.; Gordon, M. S.; Steckler, R.; Truhlar, D. G. *J. Phys. Chem.* **1989**, *93*, 5107−5119.
(54) Fernández-Ramos, A.; Truhlar, D. G. *J. Chem. Phys.* **2001**, *114*, 1491−1496.